Methionine Oxidation Interferes with Conversion of the Prion Protein into the Fibrillar Proteinase K-Resistant Conformation†

Leonid Breydo,‡ Olga V. Bocharova,‡,§ Natallia Makarava,‡ Vadim V. Salnikov,‡,|| Maighdlin Anderson,‡ and Ilia V. Baskakov*,‡,⊥

Medical Biotechnology Center, University of Maryland Biotechnology Institute, and Department of Biochemistry and Molecular Biology, University of Maryland School of Medicine, Baltimore, Maryland 21201

Received July 14, 2005; Revised Manuscript Received September 20, 2005

ABSTRACT: In recent studies, we developed a protocol for in vitro conversion of full-length mouse recombinant PrP (Mo rPrP23−230) into amyloid fibrils [Bocharova et al. (2005) *J. Mol. Biol. 346*, 645−659]. Because amyloid fibrils produced from recombinant Mo PrP89−230 display infectivity [Legname et al. (2004) *Science 305*, 673−676], polymerizatiom of rPrPs in vitro represents a valuable model for elucidating the mechanism of prion conversion. Unexpectedly, when the same conversion protocol was used for hamster (Ha) rPrP23−231, we experienced substantial difficulties in forming fibrils. While searching for potential reasons of our failure to produce fibrils, we probed the effect of methionine oxidation in rPrP. We found that oxidation of methionines interferes with the formation of rPrP fibrils and that this effect is more profound for Ha than for Mo rPrP. To minimize the level of spontaneous oxidation, we developed a new protocol for rPrP purification, in which highly amyloidogenic Ha rPrP with minimal levels of oxidized residues was produced. Furthermore, our studies revealed that oxidation of methionines in preformed fibrils inhibited subsequent maturation of fibrils into proteinase K-resistant PrP^{Sc}-like conformation (PrP-res). Our data are consistent with the proposition that conformational changes within the central region of the protein (residues 90−140) are essential for adopting PrP-res conformation and demonstrate that methionine oxidation interferes with this process. These studies provide new insight into the mechanism of prion polymerization, solve a long-standing practical problem in producing PrP-res fibrils from full-length PrP, and may help in identifying new genetic and environmental factors that modulate prion disease.

Misfolding of prion protein (PrP)[1] is believed to be the cause of several fatal neurodegenerative diseases that can be familial, sporadic, or infectious (*1*). The "protein-only" hypothesis postulates that in the case of infectious diseases a misfolded polymeric isoform of PrP (PrP^{Sc}) serves as a transmittable agent that propagates itself by the autocatalytic conversion of the normal cellular isoform of PrP (PrP^{C}) (*2*). Progression of the disease may be influenced by many genetic and environmental factors. Here we have focused on one of these factors, oxidation of PrP by a reactive oxygen species.

Proteins are important targets for various oxidants due to their abundance in biological systems and low oxidation potential. Increased protein oxidation seems to be linked to several neurodegenerative diseases such as Alzheimer's (*3*), Parkinson's disease (*4*), amyotrophic lateral sclerosis (*5*), and prion diseases (*6*). The cellular function of the normal isoform of the prion protein (PrP^{C}) still remains uncertain (*7*); however, several potential functions including the cellular response to oxidative stress have been proposed (*6*, *8*, *9*). Both PrP-depleted cells (*10*, *11*) and brain tissues of mice with ablated PrP genes (*6*, *12*) show increased protein oxidation and decreased activities of antioxidant enzymes. If PrP^{C} indeed plays a role in neutralizing oxidative stress, the protein should be exposed to reactive oxygen species.

Methionines are among the most easily oxidized amino acid residues in proteins (*13*) and are believed to serve as scavengers for various oxidants (*14*). The degree of oxidation of methionines in vivo is controlled by the balance of the production of reactive oxygen species and the reduction of methionine sulfoxide back to methionine by methionine sulfoxide reductases. Activities of many antioxidant enzymes are altered in scrapie-infected cells (*15*, *16*) and animals (*17*, *18*). Furthermore, cultured cells infected with PrP^{Sc} are more susceptible to oxidative stress (*15*, *16*). Copper and iron balance is also disrupted in the scrapie-infected brain cells (*19*−*21*). Different levels of methionine oxidation in scrapie cells compared to normal cells are likely to have an effect on the progression of the disease by influencing the physical properties of PrP.

† This work was supported by National Institutes of Health Grant NS045585 to I.V.B.

* To whom correspondence should be addressed. Phone: 410-706-4562. Fax: 410-706-8184. E-mail: Baskakov@umbi.umd.edu.

‡ University of Maryland Biotechnology Institute.

§ Present address: Institute of Bioorganic Chemistry, Russian Academy of Sciences, Moscow 117997, Russia.

|| Present address: Kazan Institute of Biochemistry and Biophysics, Russian Academy of Sciences, Kazan, Russia 420111.

⊥ University of Maryland School of Medicine.

[1] Abbreviations: PrP, prion protein; rPrP, recombinant full-length prion protein; PrP^{C}, cellular isoform of the prion protein; PrP^{Sc}, disease-associated isoform of the prion protein; PrP-res, proteinase K-resistant form of the prion protein; Mo, mouse; Ha, hamster; ThT, thioflavin T; PK, proteinase K; GSSG, glutathione disulfide; GdnHCl, guanidine hydrochloride.

10.1021/bi051369+ CCC: $30.25
Published on Web 11/05/2005

Recombinant PrP has proved very useful as a model for studying prion replication. We have previously shown that mouse (Mo) rPrP89−230 can be converted to amyloid fibrils that induced transmissible prion disease in transgenic mice overexpressing the same protein (*22*, *23*). Our recent studies demonstrated that full-length Mo recombinant PrP (Mo PrP23−230) can be easily converted to amyloid fibrils in vitro (*24*). Unexpectedly, when the same conversion protocol was used for hamster recombinant PrP (Ha PrP23−231), we experienced substantial difficulties in forming fibrils. Because oxidation of methionine residues often inhibits protein fibril formation, we investigated the effect of protein oxidation on formation of amyloid fibrils from Ha and Mo rPrPs. We have observed that, for both Ha and Mo rPrPs, oxidation of methionines disrupted elongation and lateral association of protofibrils into fibrils. To reduce spontaneous oxidation of Ha rPrP, we have developed a new protocol for purification that yields highly amyloidogenic Ha rPrP with a minimal level of spontaneous oxidation. Furthermore, oxidation of methionines in preformed fibrils inhibited structural maturation of fibrils to the PrP^{Sc}-like conformation. Structural changes in the central region of the protein (∼90−140) caused by methionine oxidation appear to be responsible for these effects. Our studies provide novel insight into the biophysical mechanism of PrP polymerization and indicate that the amyloidogenic propensity of PrP^{C} might be regulated by the level of oxidative stress.

MATERIALS AND METHODS

Protein Expression, Purification, and Conversion. Mo and Ha full-length recombinant PrPs were expressed and purified as described earlier (*24*) with the following modifications. For solubilization of inclusion bodies and purification on an IMAC column, β-mercaptoethanol was replaced with 10 mM reduced glutathione. To eliminate reduced glutathione after IMAC purification, the pooled fraction containing rPrP was subjected to gel filtration on a HiPrep 26/10 column (Amersham Biosciences), equilibrated with the oxidation buffer (6 M urea, 100 mM Tris-HCl, pH 7.5). After gel filtration the rPrP solution was diluted to a concentration of 0.3 mg/mL with the same buffer, supplemented with 5 mM EGTA and 0.2 mM oxidized glutathione, and left overnight for oxidation to proceed to completion. All following steps were as described previously (*24*). The purified rPrP was confirmed by SDS−PAGE and electrospray mass spectrometry to be a single species with an intact disulfide bond. In vitro refolding of rPrP to the α-helical form and to amyloid fibrils was performed as previously descibed (*24*).

Monitoring the Kinetics of Amyloid Formation. The effect of protein oxidation on the kinetics of amyloid formation was monitored using an automated format as described earlier (*25*) with modifications. Stock solutions of Mo rPrP23−230 or Ha rPrP23−231 (130 μM) in 6 M GdnHCl were diluted to a final protein concentration of 1 μM and incubated in 20 mM sodium acetate buffer (pH 5.0) and 2 M GdnHCl in a reaction volume of 0.18 mL in 96-well plates in the presence of ThT (10 μM). The 96-well plates were covered by ELAS septum sheets (Spike International) and incubated at 37 °C with continuous shaking at 900 rpm in a Fluoroskan Ascent CF microplate reader (Thermo Labsystems). Kinetics of fibril formation was monitored by bottom reading of fluorescence intensity every 10 min using 444 nm excitation and 485 nm emission filters. Every set of measurements was performed in triplicate, and the results were averaged.

Protein Oxidation with Hydrogen Peroxide. In a typical experiment, the α-helical form (0.3 mg/mL) or the amyloid fibrils (0.1 mg/mL) of rPrP were treated with hydrogen peroxide (10 mM) at 37 °C for 1 h in 10 mM sodium acetate (pH 5). The reaction was then quenched by adjusting the pH to 7.5 with Tris-HCl buffer (final concentration 0.1 M) and adding 5 μg/mL catalase. For mass spectrometry analysis the resulting solution was immediately dialyzed against 10 mM ammonium acetate, pH 5.5.

Protein Oxidation with Copper(II)/Ascorbate. In a typical experiment, the α-helical form (0.3 mg/mL) or the amyloid fibrils (0.1 mg/mL) of rPrP were treated with copper(II) chloride (10 μM) and sodium ascorbate (10 mM) at 37 °C for 1 h in 50 mM Hepes (pH 7.2). The reaction was then quenched by adjusting the pH to 4 with acetate buffer (final concentration 0.2 M) and adding 0.1 M thiourea. For mass spectrometry analysis the resulting solution was immediately dialyzed against 10 mM ammonium acetate, pH 5.5.

Mass Spectrometry. In a typical experiment, samples dialyzed against 10 mM ammonium acetate, pH 5.5, were diluted to 0.1 μg/μL in 1:1 water:methanol containing 1% acetic acid. The solution was directly injected at 10 μL/min into a Waters ZMD single quadrupole mass spectrometer operated in positive ion mode. The instrument acquired full scan mass spectra (m/z 500−2000) every second for 5 min.

FTIR Spectroscopy. FTIR spectra were measured with a Bruker Tensor 27 FTIR instrument (Bruker Optics, Bullerica, MA) equipped with a MCT detector cooled with liquid nitrogen. Each sample (10 μL in 10 mM sodium acetate, pH 5.0) was loaded into a BioATR II cell. A total of 1024 scans at 2 cm^{-1} resolution were collected for each sample under constant purging with nitrogen. Spectra were corrected for water vapor, and background spectra of the same buffer were subtracted. The bands were resolved by Fourier self-deconvolusion in the Opus 4.2 software package using a Lorentzian line shape and parameters equivalent to 13 cm^{-1} bandwidth at half-height and resolution enhancement factor of 2.4.

Maturation of Amyloid Fibrils and Proteinase K Digestion. Preformed rPrP fibrils were dialyzed from denaturants and heated in a water bath at 80 °C in 100 mM Tris-HCl buffer (pH 7.5) and 0.05% Triton X-100 for 10 min. The solution was then spun down in a top microfuge for 2 s to restore the original volume.

The amyloid fibrils of rPrP (0.1 mg/mL, 10 μL) were treated with PK at 37 °C for 1 h in 100 mM Tris-HCl buffer (pH 7.5, 1:50 PK:rPrP ratio). Digestion was stopped by quenching with PMSF (2 mM), followed by addition of 4× sample buffer and 9 M urea to the final urea concentration of 2.25 M. Samples were heated at 95 °C for 15 min and analyzed by SDS−PAGE on precast 12% NuPage gels (Invitrogen) followed by silver staining.

Electron Microscopy and Epifluorescence Microscopy. Negative staining was performed on formvar-coated 200-mesh grids coated with 0.01% poly(L-lysine) solution prior to staining. The samples were adsorbed for 30 s, washed with 0.1 and 0.01 M ammonium acetate for 5 s each, stained with freshly filtered 2% uranyl acetate for 30 s, dried, and then viewed in a Zeiss EM 10 CA electron microscope. Epi-

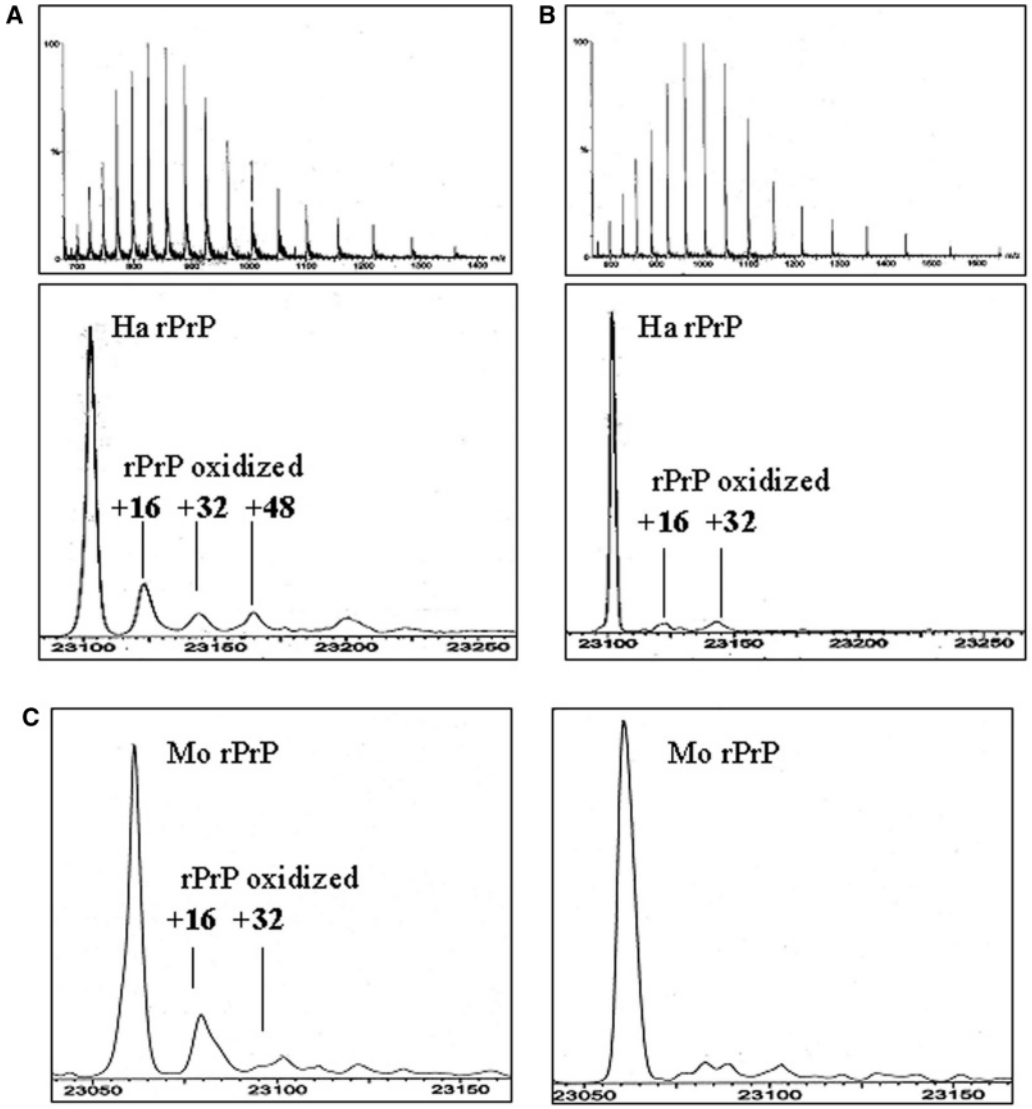

FIGURE 1: The modified purification procedure decreases oxidation of Ha rPrP. ESI-MS spectra (top panels) and their deconvolution (bottom panels) for Ha rPrP23−231 purified using original (A) and modified (B) procedures show a significantly smaller amount of oxidized rPrP in the protein obtained using the modified procedure. (C) Deconvolution of ESI-MS spectra for Mo rPrP23−230 purified using original (left panel) and modified (right panel) procedures. Oxidized rPrP species are characterized by 16, 32, or 48 Da increments in molecular mass, consistent with the incorporation of one, two, or three atoms of oxygen, respectively.

fluorescence microscopy of amyloid fibrils was performed using staining with thioflavin T as described earlier (*26*).

Atomic Force Microscopy. The samples were imaged with a PicoSPM LE AFM (Molecular Imaging, Phoenix, AZ), operating in MAC (alternating magnetic field) AFM mode and using a MAC II silicon cantilever with a tip radius <7 nm and a spring constant of 2.8 N/m. Each sample was imaged in situ using a liquid cell (Molecular Imaging, Phoenix, AZ) in which the fibrils were immersed in buffer (10 mM sodium acetate, pH 5.0). Samples were deposited on a glass coverslip (22 mm circumference; Fisherbrand), left to adhere for 3 min, and washed three times with filtered ultrapure H_2O. The slide was then placed in the fluid cell, and the samples were immersed in 200 μL of 10 mM sodium acetate buffer. The imaging was preformed at a scan rate of 1.0 line/s and a drive frequency of 25−30 kHz. All images were captured as 512 × 512 pixel scans and saved as raw image data. Images were processed in SPIP software (Image Meteorology A/S, Version 3.2.2.0). Each image was subjected to a first degree LMS fit, and then the background was isolated and subjected to a further third degree LMS fit.

RESULTS

We have previously shown that Mo rPrP23−230 can be efficiently converted in vitro into amyloid fibrils (*24*). However, when we attempted the same conversion with Ha rPrP23−231, the reaction proceeded sluggishly, with a long lag phase and a significantly lower yield as determined by ThT binding assay (data not shown). This was quite surprising since these proteins have very similar sequences and similar propensities to form PrP^{Sc} as seen from the facile propagation of many TSE strains in hamsters and mice. Changes in the reaction conditions (pH, denaturant concentrations) did not result in a significant improvement (data not shown).

We then turned our attention to chemical modification of PrP as a possible cause of the problems. Recombinant proteins are often oxidized during expression and purification. Fibril formation from other amyloidogenic proteins, for

example, Aβ (*27*−*29*) and α-synuclein (*30*, *31*), is known to be affected by oxidation of certain residues in the protein. Although our purification procedure yielded Ha rPrP free from other protein impurities, a significant fraction of protein (up to 30%) contained oxidized residues as judged from ESI-MS (Figure 1 A). Therefore, we decided to optimize the purification protocol in order to minimize protein modification.

Modified Purification Procedure Minimizes Oxidation of rPrP and Facilitates Fibril Formation. Our initial purification protocol consisted of protein purification by IMAC on a Ni-NTA column in the presence of 10 mM β-mercaptoethanol and 6 M urea (*24*). Disulfide bonds were formed by oxidation during dialysis against 6 M urea at pH 7.5 after IMAC purification overnight. The protein was then further purified by reverse-phase HPLC. Under conditions of oxidative refolding, disulfide bond formation was dependent on trace metal-mediated oxidation that could also impact oxidation of other amino acids (*13*, *32*).

We modified the purification procedure by introducing oxidized glutathione (GSSG) as an oxidizing agent for the formation of the disulfide bond instead of trace metal ions. Reduced glutathione was used as a reducing agent during IMAC purification instead of β-mercaptoethanol, and it was removed by gel filtration prior to the oxidation step. This modified procedure produced protein with much lower levels of oxidation (∼5%) (Figure 1B,C). We compared amyloid fibril formation from full-length Mo and Ha rPrPs purified by the old and new procedures. While there were no significant differences for Mo rPrP in either fibril formation kinetics or the appearance of the fibrils, it was not the case for Ha rPrP. As judged from EM, AFM performed in a liquid cell, and epifluorescence microscopy, Ha rPrP with a higher level of oxidation (old protocol) produced short fibrils (up to 1 μm long), often bent and covered with small nonfibrillar aggregates (Figure 2). Ha rPrP produced by the modified purification procedure formed amyloid fibrils with up to a 5-fold higher yield by ThT binding assay. Fibrils were long (up to 8 μm) and showed a more complex substructure (Figure 2). Apparently, even a relatively small percentage of oxidized protein in the preparation of Ha rPrP had deleterious effect on fibril formation from this protein. One can hypothesize that oxidation affected amino acid residues that are critical for the fibril formation from Ha rPrP.

Oxidation of rPrP with H_2O_2 and Cu/Ascorbate. Susceptibility of different amino acid residues to spontaneous oxidation varies to a large extent (*13*, *32*). Here we have specifically focused on oxidation of methionines since it is known that methionines in PrP are especially prone to oxidation (*33*, *34*). Furthermore, fibril formation from the PrP peptide 106−126 was inhibited by methionine oxidation (*35*). Mo and Ha rPrP differ somewhat in number and location of methionine residues (Figure 3); therefore, the effect of oxidation on amyloid formation from these proteins is likely to be different.

Treatment of the protein with H_2O_2 is a common method to specifically oxidize methionine residues (*36*). It has been reported that reaction of H_2O_2 with Ha rPrP29−231 resulted in rapid oxidation of multiple methionine residues and that the residues within the central region of rPrP (90−140) were especially susceptible to oxidation under these conditions (*33*). We have oxidized Ha and Mo rPrPs with H_2O_2 (10 mM) at pH 5 and followed the oxidation kinetics by ESI-MS (Figure 4A). We observed rapid oxidation of three to four residues in both Ha and Mo rPrP (Figure 4B). However, oxidation of Ha rPrP proceeds faster and to a somewhat higher degree (Figures 4B and 5A), which is not surprising since the solvent-exposed region of Ha rPrP contains three more methionines than that of Mo rPrP (Met109, Met112, and Met139, Figure 3).

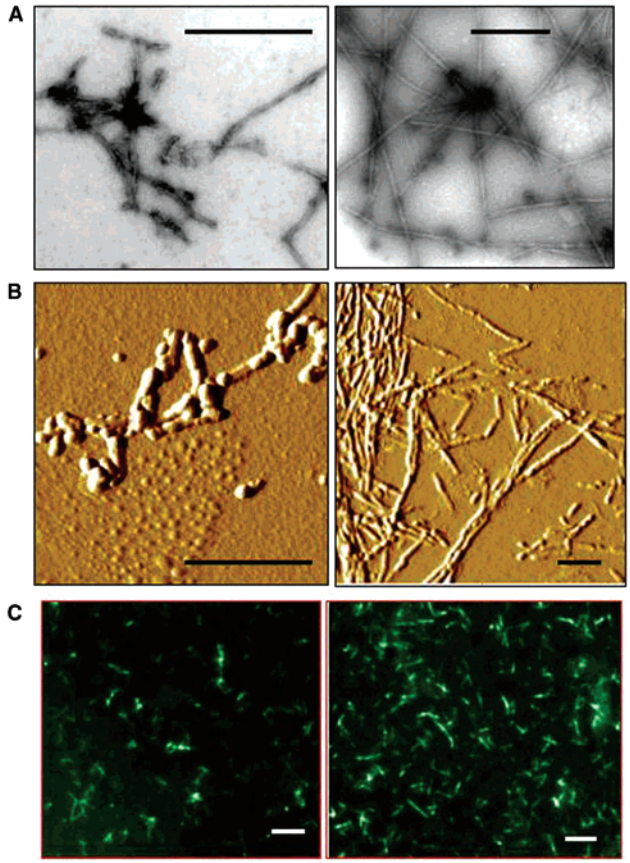

FIGURE 2: Fibrils produced from Ha rPrP purified using original (left panels) and modified (right panels) purification procedures were examined by (A) electron microscopy, (B) atomic force microscopy, and (C) epifluorescence microscopy. Fibrils were strained with 10 μM thioflavin T for epifluorescence microscopy. Fibrils formed by Ha rPrP produced by the modified procedure were longer and showed more complex substructure. Scale bars = 0.5 μm for panels A and B and 2 μm for panel C.

To check whether oxidation of other amino acids may also impact fibril formation from rPrP, we subjected rPrP to metal-catalyzed oxidation (Figure 4C). This reaction involves reduction of O_2 to $^{\bullet}OH$ by Cu(II) or Fe(III) in the presence of a reducing agent such as ascorbate. Hydroxyl radicals formed in this reaction oxidize amino acid residues located near the reaction site. Previous studies by Levine and coworkers have shown that oxidation by this method primarily affected histidines and aromatic amino acid residues in rPrP that are in close proximity to copper-binding sites (*37*). When we performed this type of oxidation (10 μM $CuCl_2$, 10 mM ascorbate, 50 mM Hepes, pH 7), Mo and Ha rPrPs oxidized at a similar rate (Figures 4C and 5B). This result was expected since copper-binding sites have similar sequences in both proteins.

H_2O_2-Induced Oxidation in rPrP Interferes with Amyloid Fibril Assembly. Next we were interested in testing whether rPrP oxidation affected fibril assembly. The effect of

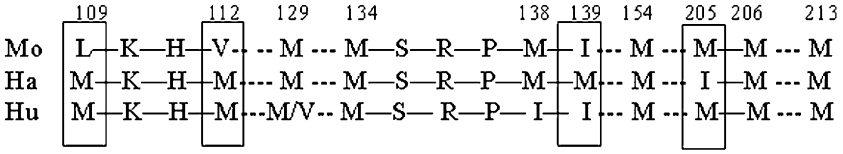

FIGURE 3: Partial sequences of Mo, Ha, and human PrPs. Positions where methionines are present in either Ha or Mo PrP but not both are highlighted.

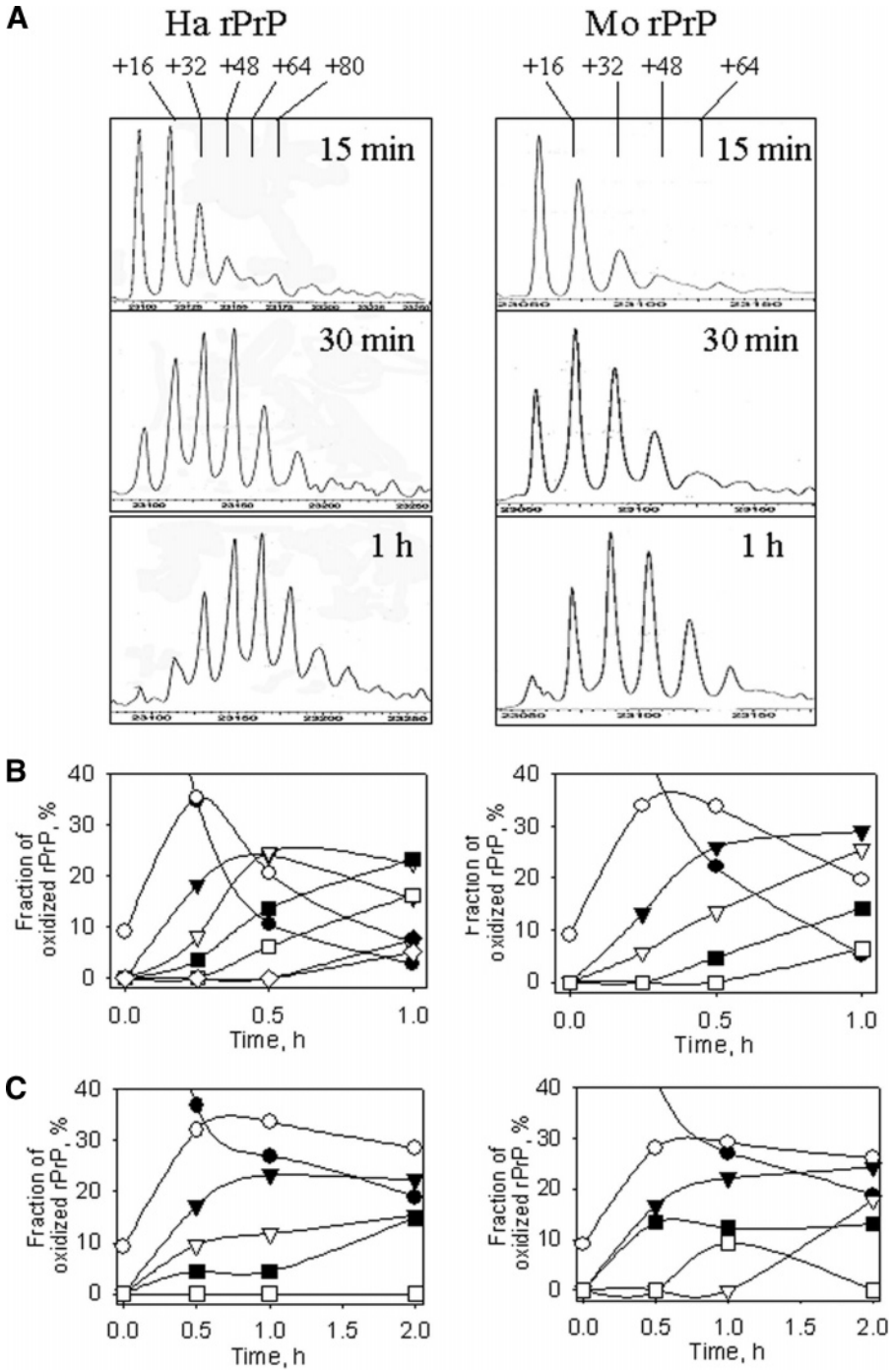

FIGURE 4: Oxidation of Ha and Mo rPrPs with H_2O_2 and Cu/ascorbate followed by ESI-MS. (A) Deconvoluted mass spectra of Ha rPrP (left panels) and Mo rPrP (right panels) oxidized with H_2O_2 (10 mM H_2O_2, 20 mM acetate, pH 5) for different periods of time. (B) Fractions of Ha rPrP (left panel) and Mo rPrP (right panel) species with none (●), one (○), two (▼), three (▽), four (■), five (□), six (◆), and seven (◇) oxidized amino acid residues per molecule observed by ESI-MS during oxidation with H_2O_2 (10 mM H_2O_2, 20 mM acetate, pH 5.0, 37 °C). (C) Fractions of Ha rPrP (left panel) and Mo rPrP (right panel) species with none (●), one (○), two (▼), three (▽), four (■), and five (□) oxidized amino acid residues per molecule observed by ESI-MS during oxidation with Cu/ascorbate (10 μM $CuCl_2$, 10 mM ascorbate, 50 mM Hepes, pH 7.0, 37 °C).

oxidation on amyloid fibril formation was investigated using a ThT binding assay and electron microscopy. The conversion of Mo and Ha rPrPs into amyloid fibrils was performed in an automated format in 96-well plates at 1 μM rPrP and

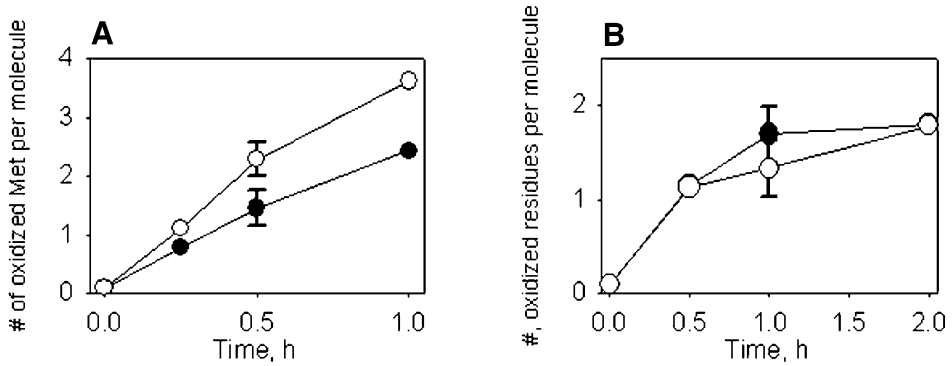

FIGURE 5: Average number of methionine residues oxidized in Ha rPrP (○) and in Mo rPrP (●) over time as determined by ESI-MS: (A) oxidation with H_2O_2 (10 mM H_2O_2, 20 mM acetate, pH 5.0, 37 °C); (B) oxidation with Cu/ascorbate (10 μM $CuCl_2$, 10 mM ascorbate, 50 mM Hepes, pH 7.0, 37 °C). Error bars represent standard deviations for triplicates.

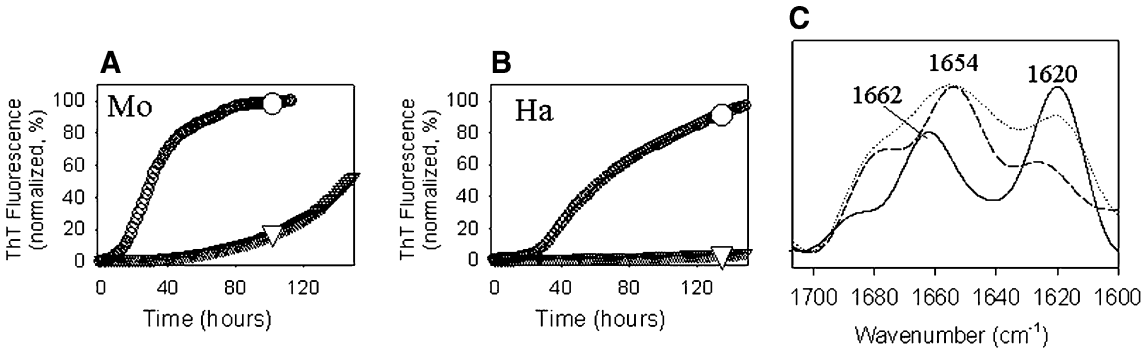

FIGURE 6: Oxidation with H_2O_2 inhibits conversion of rPrP to amyloid fibrils. The kinetics of fibril formation from 1 μM Mo rPrP (A) and Ha rPrP (B) before (○) and after (▽) oxidation with H_2O_2 (10 mM H_2O_2, 20 mM acetate, pH 5.0, 1 h, 37 °C). The conversion reactions were carried out using the automated format at 37 °C in 50 mM MES buffer (pH 6.0) and 2 M GdnHCl and monitored by ThT fluorescence. Every set of measurements was performed in triplicate, and the results were averaged. (C) FTIR spectra show that conversion of the oxidized Mo rPrP to the fibrillar isoform is incomplete: fibrils of Mo rPrP (solid line), monomeric α-helical isoform of Mo rPrP (dashed line), and fibrils produced from H_2O_2-oxidized Mo rPrP (dotted line). The sample of predominantly α-helical rPrP contained approximately 15% β-sheet-rich oligomer (peak at 1625 cm^{-1}), as assessed by size exclusion chromatography (*62*).

monitored by ThT fluorescence (see Materials and Methods). At pH 6 the reaction displayed a lag phase of 9 and 20 h for Mo and Ha rPrP, respectively (Figure 6A,B). Fibril formation from H_2O_2-oxidized rPrPs proceeded with a much longer lag phase (∼60 h for Mo and >120 h for Ha) and at 40−90% lower final ThT fluorescence compared to nonoxidized proteins (Figure 6A,B). These data demonstrate that the oxidation of methionines inhibits the formation of amyloid fibrils and that this effect is more profound for Ha rPrP than for Mo rPrP. On the other hand, oxidation to a similar level of either Ha or Mo rPrP with Cu(II)/ascorbate (10 μM $CuCl_2$, 10 mM ascorbate, 1 h, 37 °C) had no significant effect (data not shown). This result is not surprising considering that oxidation with Cu(II)/ascorbate targets primarily histidines and aromatic amino acid residues located outside of the amyloidogenic region of PrP.

To characterize the fibrils formed from the H_2O_2-oxidized PrPs in more detail, the products were investigated by EM and FTIR. As judged by EM, fibrils formed from oxidized Ha and Mo rPrPs were markedly different from those obtained from nonoxidized PrPs (Figure 7, panel 8). In the absence of H_2O_2-induced oxidation, Mo rPrP produced long straight ribbonlike fibrils characterized by complex ultrastrucuture (Figure 7, panels 1−4). Each fibril was composed of several protofilaments assembled into nontwisted or occasionally twisted structures. In the preparation of fibrils from the H_2O_2-oxidized Mo rPrP we also observed ribbonlike fibrils composed of several protofilaments with a less

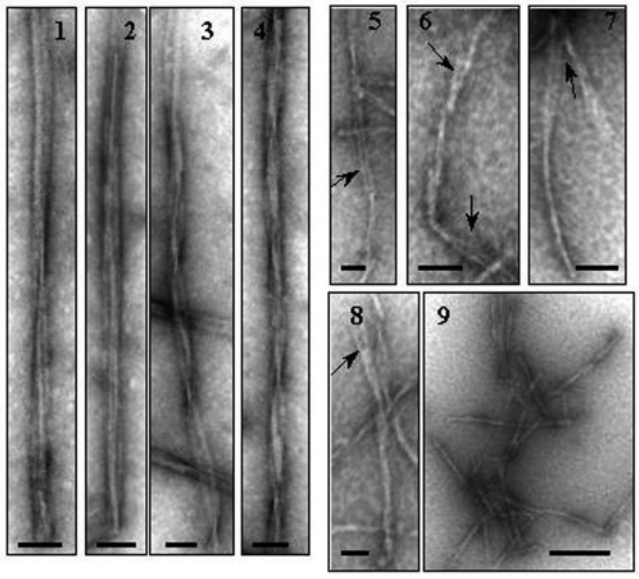

FIGURE 7: Electron micrographs of fibrils obtained from Mo rPrP (panels 1−4) and oxidized Mo rPrP (panels 5−9). Fibrils produced from oxidized Mo rPrP often displayed bending, fragmentation, or splitting of protofibrils as indicated by arrows. Oxidation was performed with 10 mM H_2O_2 for 1 h at 37 °C in 20 mM acetate buffer (pH 5.0). Fibrils were formed at 37 °C in 50 mM MES buffer (pH 6.0) and 2 M GdnHCl. Scale bars are 50 nm for panels 1−8 and 200 nm for panel 9.

complex ultrastructure (Figure 7, panels 5−9). Ribbons were unusually short, had an irregular twisting pattern, and often

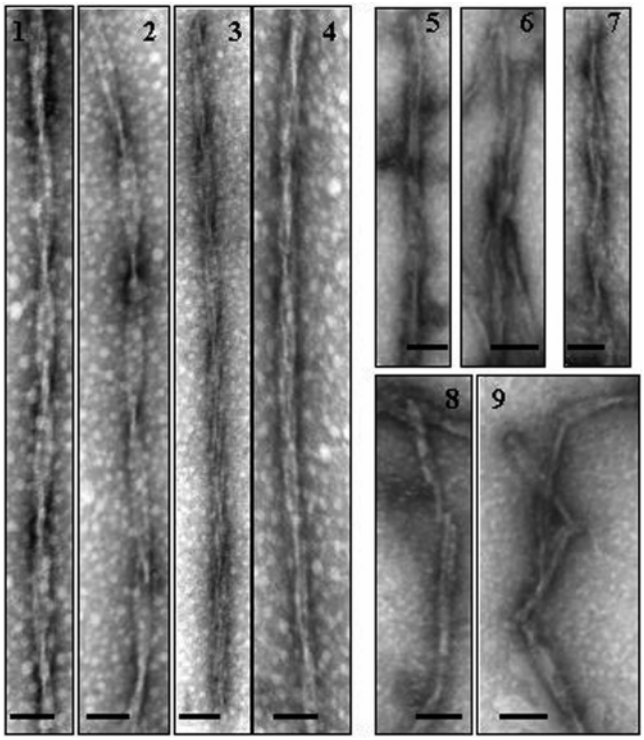

FIGURE 8: Electron micrographs of fibrils obtained from Ha rPrP (panels 1−4) and oxidized Ha rPrP (panels 5−9). Fibrils produced from oxidized Ha rPrP displayed an irregular twisting pattern, bending, and fragmentation. Oxidation was performed with 10 mM H_2O_2 for 1 h at 37 °C in 20 mM acetate buffer (pH 5.0). Fibrils were formed at 37 °C in 50 mM MES buffer (pH 6.0) and 2 M GdnHCl. Scale bars = 50 nm.

displayed bending, fragmentation, or splitting of the protofilaments. Splitting could be seen at the fibrillar ends and also along the fibrils. The unusually short length of the fibrils suggests early termination of elongation, while splitting of protofibrils may be indicative of the incomplete assembly of protofilaments into fibrils. Fibrils produced from oxidized Ha rPrP had similar features, a possible indication of incomplete assembly (Figure 8, panels 5−9). Clearly, the assembly of protofilaments into fibrils was disrupted by methionine oxidation.

To test the impact of methionine oxidation on the yield and secondary structure of amyloid fibrils, we employed FTIR spectroscopy. FTIR spectra of amyloid fibrils formed from Mo rPrP showed a major band at 1620 cm^{-1}, a characteristic of β-sheet structures with strong intermolecular hydrogen bonds, and a band at 1662 cm^{-1} that can be largely assigned to loop components (1660−1666 cm^{-1} region) with possible contributions from β-turns (1670−1680 cm^{-1} region) and α-helices (1650−1660 cm^{-1} region) (Figure 6C). FTIR spectra of fibrils formed from oxidized Mo rPrP showed a major band at 1654 cm^{-1} indicating a high percentage of α-helices and a smaller band at 1620 cm^{-1} that corresponds to intermolecular β-sheets. The intensities of bands at 1675−1685 cm^{-1} (corresponding mostly to β-turns) increased relative to that observed in fibrils formed from nonoxidized protein.

FTIR spectra show that the conversion of H_2O_2-oxidized Mo rPrP to the fibrillar isoform is incomplete and a high percentage of the protein remains in an α-helical conformation. The effect of oxidation on the conversion of Ha rPrP into amyloid fibrils was similar (data not shown). Taken

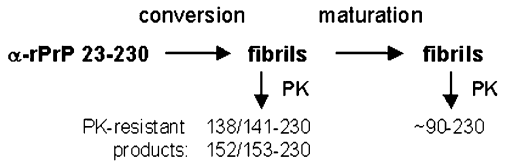

FIGURE 9: Diagram illustrating the major steps of in vitro polymerization of rPrP into the fibrillar PrP^{Sc}-like conformation. The first step referred to as conversion results in the formation of amyloid fibrils, in which region 23−∼140 adopts a PK-sensitive conformation (*38*). The second step referred to as maturation leads to conformational rearrangements in which region ∼90−140 adopts a PK-resistant conformation, while the N-terminal region 23−∼90 still maintains a PK-sensitive form.

together, our data illustrate that oxidation of methionine residues in full-length rPrPs interferes with its conversion to the amyloid fibrils. Both elongation of the protofibrils and lateral association of protofibrils into fibrils were affected by oxidation.

Oxidation of Preformed Fibrils Inhibits Their Maturation to the PrP^{Sc}-like Conformation. In vivo oxidation may be even more prevalent in PrP^{Sc} compared to PrP^{C} because PrP^{Sc} persists in the body for a longer time and thus has a higher chance of being oxidized. We investigated the effects of oxidation of preformed amyloid fibrils in order to see whether oxidation of methionines disturbs the structure of the fibrils. Oxidation with hydrogen peroxide did not change the appearance of fibrils by EM (data not shown). FTIR spectra of oxidized fibrils were also quite similar to the spectra before oxidation (data not shown). We conclude that methionine oxidation in preformed fibrils does not affect their structural integrity.

We have previously observed that amyloid fibrils of rPrP generated in vitro had an atypically short PK-resistant core of 8−12 kDa, which consists of residues 138−230, 152−230, and 162−230 (*38*). These short PK-resistant fragments are similar to the fragments identified in brains of CJD patients (*39*) but are notably different from the PK-resistant core generated from classical PrP^{Sc}. Recently, we found that brief heating at 80 °C or prolonged incubation at 37 °C of preformed amyloid fibrils in the presence of a mild detergent resulted in the extension of the PK-resistant core from 8−12 to 16 kDa. The new PK-resistant fragment of 16 kDa could be stained with Fab P and Fab R1, specific to residues 96−105 and 225−230, respectively, but not with polyclonal antibodies Ab 79−97, specific to residues 79−97 (data not shown). The process of temperature-induced elongation of the PK-resistant core will be referred to as maturation (Figure 9). Upon maturation the PK-resistant core of amyloid fibrils becomes similar to that of classical PrP^{Sc}. This suggests that maturation may be due to rearrangement of the central region of PrP (residues 90−140) via a process similar to domain swapping (*40*). Similar conformational rearrangement triggered by mild detergents has been observed previously for Bcl-2 protein (*41*).

Because the central region 90−140 of Mo and Ha rPrPs contains three and six Met residues, respectively (Figure 3), we were interested in determining whether oxidation of preformed fibrils interferes with their ability to adopt a PrP^{Sc}-like conformation upon maturation. In the fibrillar form the region 90−138 is PK-sensitive, ensuring that it should be accessible to solvent, at least in part. We oxidized Mo and Ha rPrP preformed fibrils with H_2O_2 (10 mM H_2O_2, 1 h, 37

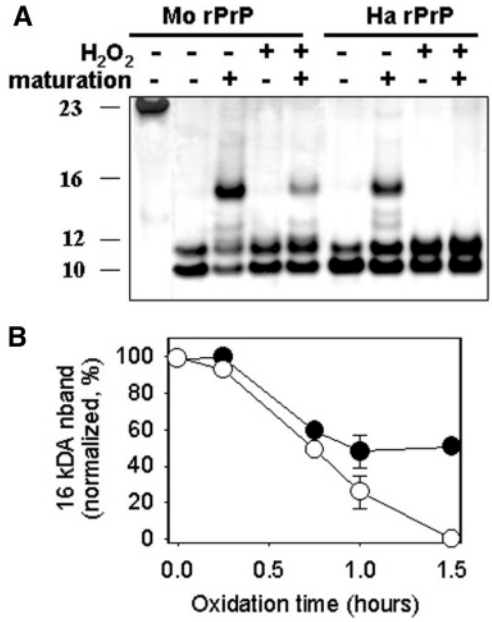

FIGURE 10: Oxidation of fibrils inhibits their maturation to the PrP^{Sc}-like conformation. (A) PK digestion (PK/rPrP ratio of 1:50 in 100 mM Tris-HCl, pH 7.5, for 1 h at 37 °C) of amyloid fibrils produced from Mo or Ha rPrPs preincubated with or without 10 mM H_2O_2 in 10 mM acetate buffer (pH 5.0) for 1 h at 37 °C. Following oxidation fibrils were subjected to the maturation procedure and PK digestion assay as described in Materials and Methods. No PK was added in lane 1. (B) Changes in intensity of the 16 kDa band vs oxidation time for the fibrils produced from Mo rPrP (●) or Ha rPrP (○). Fibrils were treated with H_2O_2 prior to maturation. Error bars represent standard deviations for triplicates.

°C), subjected them to the maturation procedure, and monitored the intensity of the 16 kDa band (residues ~90−230) after proteinase K digestion (Figure 10A). With an increase in the oxidation time, the intensity of the 16 kDa band generated upon maturation decreased by 50% for Mo rPrP and to undetectable levels for Ha rPrP (Figure 10B). The higher efficacy of H_2O_2 treatment to counteract the maturation of fibrils into the PrP^{Sc}-like conformation in Ha rPrP correlates well with the larger number of Met residues located within the central region of Ha rPrP.

Attenuation of the maturation effect can be explained by a change in the physical properties of the central region of PrP (90−140) involved in the maturation. Upon oxidation, hydrophobic methionine side chains convert into highly polar methionine sulfoxides. While this alteration appears to have no significant effect on structural integrity of preformed fibrils, it significantly reduces the ability of fibrils to mature and adopt a PrP^{Sc}-like conformation. This result is consistent with our previous observations that the C-terminal region (residues 138−230) composes the PK-resistant core and accounts for the structural integrity of fibrils (*38*). The data presented here confirm that while the central region of PrP (residues 90−138) may not be a part of the β-sheet-rich core of the fibrils, it is definitely important for conformational rearrangements that lead to the maturation of fibrils into the PrP^{Sc}-like conformation.

DISCUSSION

In the current study, we have investigated the effects of methionine oxidation on in vitro conversion of Mo and Ha rPrPs into the amyloid fibrils. We demonstrated that oxidation of methionine residues in rPrP interferes with the conversion of the protein to the fibrillar form and disrupts maturation of fibrils into the PrP^{Sc}-like PK-resistant conformation. These studies provided mechanistic insight into the possible role of oxidation in modulating prion conversion. The results of our experiments are consistent with literature data showing that oxidation of methionine residues inhibits fibril formation from other amyloidogenic proteins such as Aβ (*27*−*29*) and α-synuclein (*30*, *31*). Our work also helps to solve a long-standing practical problem in producing amyloid fibrils from full-length rPrP in vitro.

Oxidation of methionines can have a drastic effect on protein structure due to a much higher polarity and lower flexibility of methionine sulfoxide compared to the methionine side chain itself (*13*, *36*). Previous investigations of oxidation of Ha rPrP have shown that methionines in the central region (residues 90−140) are most susceptible to oxidation by H_2O_2 (*33*). Oxidation of PrP with H_2O_2 would then result in alteration of the physical properties of the central region of PrP that could impact polymerization of PrP into disease-related amyloid conformation. We found that oxidation of rPrP with H_2O_2 but not with Cu/ascorbate interferes with amyloid formation. As supported by our data, the low efficacy of conversion is due to early termination of elongation and interference with lateral assembly of profilaments into fibrils.

Several structural models of PrP^{Sc} have been proposed recently (*42*−*46*). These models disagree with respect to what regions of PrP adopt a β-sheet-rich conformation upon conversion into the PrP^{Sc} form. The model proposed by Prusiner and co-workers based on EM imaging of 2D crystals of PrP^{Sc} involves conversion of residues 89−175 to a β-helical conformation with the rest of the C-terminus remaining α-helical (*42*, *43*). Molecular dynamics simulations by DeMarco and Daggett (*44*) and by Stork et al. (*47*) are in overall agreement with this model. The model by DeMarco and Daggett suggests that residues 114−140 and 157−165 are converted to the β-structure at low pH (*44*). On the other hand, a simulation by Thirumalai suggests that residues 172−224 are converted to a β-sheet-rich conformation in the intermediate PrP* form (*45*). Both the central (residues 90−140) and the C-terminal (residues 177−230) regions are considered important for infectivity of PrP^{Sc} (*48*, *49*), but an exact role for these regions at different steps in the prion conversion is unclear. Our previous data are consistent with the model where C-terminal residues of PrP (~160−230) are converted to the β-sheet-rich, PK-resistant conformation in the amyloid form (*38*).

The central region of PrP (90−140) is PK-sensitive in amyloid fibrils, arguing that the fibrils generated in vitro resemble the protease-sensitive form of PrP^{Sc} (*50*, *51*). Upon fibril maturation this region becomes PK-resistant, so the mature fibrils are similar in this regard to PrP-res or "classical" PrP^{Sc} (Bocharova and Baskakov, unpublished data; Figure 9). Our data illustrate that the region 90−140 plays a key role in maturation of fibrils and their transformation into PrP^{Sc}-like conformation; however, it is not directly involved in the formation of the amyloid core. The situation is similar for the middle (M) region of Sup35 yeast prion that is not a part of the amyloid core but is important for prion propagation (*52*, *53*). As evident from the present study,

oxidation of methionine residues in preformed fibrils interferes with the ability of these fibrils to adopt a PrP-res conformation. This inhibition may be due to perturbation of hydrophobic interactions required for the rearrangement of the central region into the PK-resistant conformation.

We also showed that oxidation of methionines in monomeric α-rPrP interferes with the assembly of amyloid fibrils themselves. If the same pattern holds in vivo, the overall effect of methionine oxidation would result in the accumulation of various intermediates on the pathway between PrP^C and PrP^{Sc}. There is significant evidence that the mature form of PrP^{Sc} may not be the most neurotoxic species. Instead, smaller oligomers of PrP and various soluble fibrillization intermediates may account for neurotoxicity. Similar mechanisms of neurotoxicity have been proposed for Alzheimer's and other amyloid diseases (*54*−*56*). Moreover, toxicity and infectivity of PrP^{Sc} are not necessarily coupled. For example, the peptide corresponding to residues 106−126 of PrP is neurotoxic but has not shown any infectivity (*57*, *58*). On the other hand, scrapie-infected transgenic mice producing PrP^C that lacks a GPI anchor propagated PrP^{Sc} but showed no clinical signs of scrapie (*59*). However, the question of whether the intermediate species formed from methionine-oxidized PrP^C are more toxic than mature PrP^{Sc} needs to be addressed in future studies.

Considering the inhibitory effect of oxidation on the conversion reaction, differences in the sequences of PrP from different species may have a significant effect on the rate of PrP^{Sc} formation. The number and susceptibility of methionine residues to oxidation determine the extent of the inhibitory effects. We have observed that more residues are oxidized in Ha rPrP than in Mo rPrP. Moreover, oxidation of Ha rPrP was more efficient in blocking maturation of the amyloid fibrils into the PrP^{Sc}-like conformation compared to Mo rPrP. This result is not surprising considering that Ha rPrP has three additional methionines within the solvent-accessible region 90−140 and, therefore, is more susceptible to oxidation than Mo rPrP. Because of polymorphisms at residue 129, human PrP has either three or four methionines in the 100−135 region but no methionines in the 135−140 region (Ha PrP has two methionines and Mo PrP has one methionine in the 135−140 region; Figure 3). Therefore, oxidation-related inhibition of polymerization of human PrP is expected to be stronger than that observed for Mo PrP but weaker than that for Ha PrP. Interestingly, when position 129 in human PrP is occupied by methionine, the age at onset of sporadic CJD is usually later than that observed in 129V patients (*60*). This fact may be explained in part by the higher susceptibility of 129M PrP^C to oxidation by reactive oxygen species and, respectively, slower conversion rate. Noteworthy, individuals with 129M PrP were shown to have better long-term memory than individuals with 129V PrP (*61*). Because 129M PrP^C would be expected to be a more efficient scavenger of reactive oxygen species than 129V PrP^C, one can hypothesize that PrP^C may account for the maintenance of long-lasting functional synapses in brain.

Our work provides the first illustration that oxidation of methionine residues has dramatic impact on polymerization of PrP into the fibrillar form. The extent to which PrP^C and PrP^{Sc} are oxidized in vivo has yet to be determined. It is not unlikely, however, that the high susceptibility of PrP to oxidation happens to be related to both cellular function of PrP^C and pathogenesis in prion diseases and, therefore, may create the missing bridge between these two processes.

REFERENCES

1. Prusiner, S. B. (1997) Prion diseases and the BSE crisis, *Science 278*, 245−251.
2. Prusiner, S. B. (1982) Novel proteinaceous infectious particles cause scrapie, *Science 216*, 136−144.
3. Perry, G., Nunomura, A., Hirai, K., Zhu, X., Perez, M., Avila, J., Castellani, R. J., Atwood, C. S., Aliev, G., Sayre, L. M., Takeda, A., and Smith, M. A. (2002) Is oxidative damage the fundamental pathogenic mechanism of Alzheimer's and other neurodegenerative diseases?, *Free Radical Biol. Med. 33*, 1479.
4. Giasson, B. I., Duda, J. E., Murray, I. V. J., Chen, Q., Souza, J. M., Hurtig, H. I., Ischiropoulos, H., Trojanowski, J. Q., and Lee, V. M. Y. (2000) Oxidative damage linked to neurodegeneration by selective α-synuclein nitration in synucleinopathy lesions, *Science 290*, 985−989.
5. Carri, M. T., Ferri, A., Cozzolino, M., Calabrese, L., and Rotilio, G. (2003) Neurodegeneration in amyotrophic lateral sclerosis: the role of oxidative stress and altered homeostasis of metals, *Brain Res. Bull. 61*, 365−374.
6. Brown, D. R. (2001) Prion and prejudice: normal protein and the synapse, *Trends Neurosci. 24*, 85−90.
7. Aguzzi, A., and Polymenidou, M. (2004) Mammalian prion biology: one century of evolving concepts, *Cell 116*, 313−327.
8. Brown, D. R., and Besinger, A. (1998) Prion protein expression and superoxide dismutase activity, *Biochem. J. 334*, 423−429.
9. Millhauser, G. L. (2004) Copper binding in the prion protein, *Acc. Chem. Res. 37*, 79−85.
10. Brown, D. R., Schulz-Schaeffer, W. J., Schmidt, B., and Kretzschmar, H. A. (1997) Prion protein-deficient cells show altered response to oxidative stress due to decreased SOD-1 activity, *Exp. Neurol. 146*, 104−112.
11. Rachidi, W., Vilette, D., Guiraud, P., Arlotto, M., Riondel, J., Laude, H., Lehmann, S., and Favier, A. (2003) Expression of prion protein increases cellular copper binding and antioxidant enzyme activities but not copper delivery, *J. Biol. Chem. 278*, 9064−9072.
12. Klamt, F., Dal-Pizzol, F., Conte da Frota, M. L., Jr., Walz, R., Andrades, M. E., sa Silva, E. G., Brentani, R. R., Izquierdo, I., and Fonseca Moreira, J. C. (2001) Imbalance of antioxidant defence in mice lacking cellular prion protein, *Free Radical Biol. Med. 30*, 1137−1144.
13. Davies, M. J. (2005) The oxidative environment and protein damage, *Biochim. Biophys. Acta 1703*, 93−109.
14. Levine, R. L., Mosoni, L., Berlett, B. S., and Stadtman, E. R. (1996) Methionine residues as endogenous antioxidants in proteins, *Proc. Natl. Acad. Sci. U.S.A. 93*, 15036−15040.
15. Milhavet, O., McMahon, H. E., Rachidi, W., Nishida, N., Katamine, S., Mange, A., Arlotto, M., Casanova, D., Riondel, J., Favier, A., and Lehmann, S. (2000) Prion infection impairs the cellular response to oxidative stress, *Proc. Natl. Acad. Sci. U.S.A. 97*, 13937−13942.
16. Fernaeus, S., and Land, T. (2005) Increased iron-induced oxidative stress and toxicity in scrapie-infected neuroblastoma cells, *Neurosci. Lett. 382*, 217−220.
17. Kim, J. I., Ju, W. K., Choi, J. H., Choi, E., Carp, R. I., Wisniewski, H. M., and Kim, Y. S. (1999) Expression of cytokine genes and increased nuclear factor-kappa B activity in the brains of scrapie infected mice, *Brain Res. Mol. Brain Res. 73*, 17−27.
18. Wong, B. S., Brown, D. R., Pan, T., Whiteman, M., Liu, T., Bu, X., Li, R., Gambetti, P., Olesik, J., Rubenstein, R., and Sy, M. S. (2001) Oxidative impairment in scrapie-infected mice is associated with brain metals perturbations and altered antioxidant activities, *J. Neurochem. 79*, 689−698.
19. Fernaeus, S., Halldin, J., Bedecs, K., and Land, T. (2005) Changed iron regulation in scrapie-infected neuroblastoma cells, *Brain Res. Brain Res. Rev. 133*, 266−273.
20. Brown, D. R. (2004) Mettalic prions, *Biochem. Soc. Symp. 71*, 193−202.
21. Rachidi, W., Mange, A., Senator, A., Guiraud, P., Riondel, J., Benboubetral, M., Favier, A., and Lehmann, S. (2003) Prion infection impairs copper binding of cultured cells, *J. Biol. Chem. 278*, 14595−14598.
22. Baskakov, I. V., Legname, G., Baldwin, M. A., Prusiner, S. B., and Cohen, F. E. (2002) Pathway complexity of prion protein assembly into amyloid, *J. Biol. Chem. 277*, 21140−21148.

23. Legname, G., Baskakov, I. V., Nguyen, H.-O. B., Riesner, D., Cohen, F. E., DeArmond, S. J., and Prusiner, S. B. (2004) Synthetic mammalian prions, *Science 305*, 673−676.
24. Bocharova, O. V., Breydo, L., Parfenov, A. S., Salnikov, V. V., and Baskakov, I. V. (2005) In vitro conversion of full length mammalian prion protein produces amyloid form with physical property of PrPSc, *J. Mol. Biol. 346*, 645−659.
25. Breydo, L., Bocharova, O. V., and Baskakov, I. V. (2005) Semiautomated cell-free conversion of prion protein: Applications for high-throughput screening of potential antiprion drugs, *Anal. Biochem. 339*, 165−173.
26. Baskakov, I. V., and Bocharova, O. V. (2005) In vitro conversion of mammalian prion protein into amyloid fibrils displays unusual features, *Biochemistry 44*, 2339−2348.
27. Hou, L., Shao, H., Zhang, Y., Li, H., Menon, N. K., Neuhaus, E. B., Brewer, J. M., Byeon, I.-J. L., Ray, D. G., Vitek, M. P., Iwashita, T., Makula, R. A., Przybyla, A. B., and Zagorski, M. G. (2004) Solution NMR studies of the A-beta(1−40) and A-beta-(1−42) peptides establish that Met35 oxidation state affects the mechanism of amyloid formation, *J. Am. Chem. Soc. 126*, 1992−2005.
28. Watson, A. A., Fairlie, D. P., and Craik, D. J. (1998) Solution structure of methionine-oxidized amyloid beta-peptide (1−40). Does oxidation affect conformational switching?, *Biochemistry 37*, 12700−12706.
29. Bitan, G., Tarus, B., Vollers, S. S., Lashuel, H. A., Condron, M. M., Straub, J. E., and Teplow, D. B. (2003) A molecular switch in amyloid assembly: Met35 and amyloid beta-protein oligomerization, *J. Am. Chem. Soc. 125*, 15359−15365.
30. Uversky, V. N., Yamin, G., Souillac, P. O., Goers, J., Glaser, C. B., and Fink, A. L. (2002) Methionine oxidation inhibits fibrillation of human a-synuclein in vitro, *FEBS Lett. 517*, 239−244.
31. Hokenson, M. J., Uversky, V. N., Goers, J., Yamin, G., Munishkina, L. A., and Fink, A. L. (2004) Role of individual methionines in the fibrillation of methionine-oxidized a-synuclein, *Biochemistry 43*, 4621−4633.
32. Stadtman, E. R., and Berlett, B. S. (1997) Reactive oxigen-mediated protein oxidation in aging and disease, *Chem. Res. Toxicol. 10*, 485−494.
33. Requena, J. R., Dimitrova, M. N., Legname, G., Teijeira, S., Prusiner, S. B., and Levine, R. L. (2004) Oxidation of methionine residues in the prion protein by hydrogen peroxide, *Arch. Biochem. Biophys. 432*, 188−195.
34. Wong, B. S., Wang, H., Brown, D. R., and Jones, I. M. (1999) Selective oxidation of methionine residues in prion proteins, *Biochem. Biophys. Res. Commun. 259*, 352−355.
35. Heegaard, P. M. H., Pedersen, H. G., Flink, J., and Boas, U. (2004) Amyloid aggregates of the prion peptide PrP106−126 are destabilised by oxidation and by the action of dendrimers, *FEBS Lett. 577*, 127−133.
36. Vogt, W. (1995) Oxidation of methionyl residues in proteins: tool, targets, and reversal, *Free Radical Biol. Med. 18*, 93−105.
37. Requena, J., Groth, D., Legname, G., Stadtman, E. R., Prusiner, S. B., and Levine, R. L. (2001) Copper-catalyzed oxidation of the recombinant SHa(29−231) prrion protein, *Proc. Natl. Acad. Sci. U.S.A. 98*, 7170−7175.
38. Bocharova, O. V., Breydo, L., Salnikov, V. V., Gill, A. C., and Baskakov, I. V. (2005) Synthetic prions generated in vitro are similar to a newly identified subpopulation of PrPSc from sporadic Creutzfeldt−Jakob disease PrP^{Sc}, *Protein Sci. 14*, 1222−1232.
39. Zou, W. Q., Capellari, S., Parchi, P., Sy, M. S., Gambetti, P., and Chen, S. G. (2003) Identification of novel proteinase K-resistant C-terminal fragments of PrP in Creutzfeldt−Jakob disease, *J. Biol. Chem. 278*, 40429−40436.
40. Liu, Y., and Eisenberg, D. (1995) 3D domain swapping: As domains continue to swap, *Protein Sci. 11*, 1285−1299.
41. Hsu, Y. T., and Youle, R. J. (1997) Nonionic detergents induce dimerization amoung members of the Bcl-2 family, *J. Biol. Chem. 272*, 13834.
42. Wille, H., Michelitsch, M. D., Guenebaut, V., Supattapone, S., Serban, A., Cohen, F. E., Agard, D. A., and Prusiner, S. B. (2002) Structural studies of the scrapie prion protein by electron crystallography, *Proc. Natl. Acad. Sci. U.S.A. 99*, 3563−3568.
43. Govaerts, C., Wille, H., Prusiner, S. B., and Cohen, F. E. (2004) Evidance for assembly of prions with left-handed b-helices into trimers, *Proc. Natl. Acad. Sci. U.S.A. 101*, 8342−8347.
44. DeMarco, M. L., and Daggett, V. (2004) From conversion to aggregation: protofibrils formation of the prion protein, *Proc. Natl. Acad. Sci. U.S.A. 101*, 2293−2298.
45. Dima, R. I., and Thirumalai, D. (2004) Probing the instabilities in the dynamics of helical fragments from mouse PrPC, *Proc. Natl. Acad. Sci. U.S.A. 101*, 15335−15340.
46. Eghiaian, F., Grosclaude, J., Lesceu, S., Debey, P., Doublet, B., Treguer, E., Rezaei, H., and Knossow, M. (2004) Insight into the PrPC→PrPSc conversion from the structures of antibody-bound ovine prion scrapie susceptibility variants, *Proc. Natl. Acad. Sci. U.S.A. 101*, 10254−10259.
47. Stork, M., Giese, A., Kretzchmar, H. A., and Tavan, P. (2005) Molecular dynamics simulations indicate a possible role of parallel b-helices in seeded aggregation of poly-Gln, *Biophys. J. 88*, 2442−2451.
48. Muramoto, T., Scott, M., Cohen, F. E., and Prusiner, S. B. (1996) Recombinant scrapie-like prion protein of 106 amino acids is soluble, *Proc. Natl. Acad. Sci. U.S.A. 93*, 15457−15462.
49. Supattapone, S., Bosque, P., Muramoto, T., Wille, H., Aagaard, C., Peretz, D., Nguyen, H.-O. B., Heinrich, C., Torchia, M., Safar, J., Cohen, F. E., DeArmond, S. J., Prusiner, S. B., and Scott, M. (1999) Prion protein of 106 residues creates an artificial transmission barrier for prion replication in transgenic mice, *Cell 96*, 869−878.
50. Safar, J., Wille, H., Itri, V., Groth, D., Serban, H., Torchia, M., Cohen, F. E., and Prusiner, S. B. (1998) Eight prion strains have PrP^{Sc} molecules with different conformations, *Nat. Med. 4*, 1157−1165.
51. Tzaban, S., Friedlander, G., Schonberger, O., Horonchik, L., Yedidia, Y., Shaked, G., Gabizon, R., and Taraboulos, A. (2002) Protease-sensitive scrapie prion protein in aggregates of heterogeneous sizes, *Biochemistry 41*, 12868−12875.
52. Krishnan, R., and Lindquist, S. (2005) Structural insight into a yeast prion illuminate nucleation and strain diversity, *Nature 435*, 765−772.
53. Liu, J. J., Sondheimer, N., and Lindquist, S. (2002) Changes in the middle region of Sup35 profoundly alter the nature of epigenetic inheritance for the yeast prion [PSI+], *Proc. Natl. Acad. Sci. U.S.A. 99*, 16446−16453.
54. Bucciantini, M., Giannoni, E., Chiti, F., Baroni, F., Formigli, L., Zurdo, J., Taddei, N., Ramponi, G., Dobson, C. M., and Stefani, M. (2002) Inherent toxicity of aggregates implies a common mechanism for protein misfolding diseases, *Nature 416*, 507−511.
55. Kayed, R., Head, E., Thompson, J. L., McIntire, T. M., Milton, S. C., Cotman, C. W., and Glabe, C. G. (2003) Common structure of soluble amyloid oligomers implies common mechanism of pathogenesis, *Science 300*, 486-489.
56. Caughey, B., and Lansbury, P. T. (2005) Protofibrils, pores, fibrils, and neurodegeneration: separating the responsible protein aggregates from the innocent bystanders, *Annu. Rev. Neurosci. 26*, 267−298.
57. Forloni, G., Angeretti, N., Chiesa, R., Monzani, E., Salmona, M., Bugiani, O., and Tagliavini, F. (1993) Neurotoxicity of a prion protein fragment, *Nature 362*, 543−546.
58. Fioriti, L., Quaglio, E., Massignan, T., Colombo, L., Stewart, R. S., Salmona, M., Harris, D. A., Forloni, G., and Chiesa, R. (2005) The neurotoxicity of prion protein (PrP) peptide 106−126 is independent of the expression level of PrP and is not mediated by abnormal PrP species, *Mol. Cell. Neurosci. 28*, 176.
59. Chesebro, B., Trifilo, M., Race, M., Meade-White, K., Teng, C., LaCasse, R., Raymond, L., Favara, C., Baron, G., Priola, S., Caughey, B., Masliah, E., and Oldstone, M. (2005) Anchorness prion protein result in infectious amyloid disease without clinical scrapie, *Science 308*, 1435−1439.
60. Parchi, P., Giese, A., Capellari, S., Brown, P., Schulz-Schaeffer, W., Windl, O., Zerr, I., Budka, H., Kopp, N., Piccardo, P., Poser, S., Rojiani, A., Streichemberger, N., Julien, J., Vital, C., Ghetti, B., Gambetti, P., and Kretzschmar, H. (1999) Classification of sporadic Creutzfeldt−Jakob disease based on molecular and phenotypic analysis of 300 subjects, *Ann. Neurol. 46*, 224−233.
61. Papassotiropoulos, A., Wollmer, M. A., Aguzzi, A., Hock, C., Nitsch, R. M., and de Quervain, D. J. (2005) The prion gene is associated with human long-term memory, *Hum. Mol. Genet.* (Epub).
62. Baskakov, I. V., Legname, G., Gryczynski, Z., and Prusiner, S. B. (2004) The peculiar nature of unfolding of human prion protein, *Protein Sci. 13*, 586−595.

BI051369+